Effect of inorganic filler type and in-situ Silane modification on lap shear strength and thermal aging durability of polyamide-cured epoxy adhesive on aluminum alloy

Nguyen Thi Ngoan[1], Pham The Long[1], Nguyen Minh Viet[2], Le The Hoai[2], Tran The Dinh[3], Dao Xuan Phuc[4], Cong Tien Dung[5, 6*]

[1]High Technology Innovation Center, Vietnam Academy of Science and Technology, 18 Hoang Quoc Viet, Nghia Do, Hanoi, Vietnam;
[2]Hanoi University of Industry, 298 Cau Dien, Tay Tuu, Hanoi, Vietnam;
[3]Institute for Technology of Radioactive and Rare Elements, 48 Lang Ha, Lang, Hanoi, Vietnam;
[4]Hanoi Open University, B101, Nguyen Hien, Bach Mai, Hanoi, Vietnam;
[5]Department of Chemistry, Hanoi University of Mining and Geology, 18 Vien Street, Dong Ngac, Hanoi, Vietnam;
[6]BSASD Research Group, Hanoi University of Mining and Geology, 18 Vien Street, Dong Ngac, Hanoi, Vietnam.
[*]Corresponding author: congtiendung@humg.edu.vn
Received 18 Mar. 2026; Revised 04 May 2026; Accepted 15 Jun. 2026; Published 25 Jun. 2026.
DOI: https://doi.org/10.54939/1859-1043.j.mst.112.2026.92-100

ABSTRACT

This study investigates the effects of inorganic filler type (ZrO_2, Al, TiO_2, TiC, WC, h-BN) and in-situ silane modification (APTMS, GPTMS, VTMS) on the lap shear strength (LSS) and thermal stability of a polyamide-cured epoxy adhesive on 6061 aluminum alloy. The optimal ZrO_2 content was 5.0 wt%, yielding an initial LSS_0 of 12.4 MPa and a 500-h thermal retention factor at 80 °C (TRF-500h) of 83.1% without silane. APTMS outperformed other silanes through a dual interfacial bonding mechanism, raising the LSS_0 to 15.6 MPa and TRF-500h to 88.5% for the ZrO_2-5.0-APTMS system. Evaluation of six filler types against dual criteria ($LSS_0 \geq 15$ MPa, TRF-500h ≥ 85%) identified h-BN, WC, ZrO_2, and TiC as qualifying systems. The h-BN-5.0-APTMS system achieved the best overall performance (TRF = 90.6%, $LSS_{500}h$ = 14.5 MPa), driven by the unique tortuosity effect and high thermal conductivity of its lamellar structure. TGA/DTG analysis confirmed higher T_5% values for all filled systems compared to the unfilled epoxy (323 °C), following the order WC (341 °C) > BN (339 °C) > TiC (337 °C) > ZrO_2 (331 °C) > Al (329 °C) > TiO_2 (325 °C) due to the oxygen diffusion barrier effect. These results guide the development of thermally durable modified adhesives for structural applications.

Keywords: Epoxy/polyamide adhesive; Inorganic filler; APTMS silane; Lap shear strength; Thermal aging.

1. INTRODUCTION

Epoxy resins cured with polyamide hardeners exhibit excellent adhesion, flexibility, and toughness, making them highly suitable for structural bonding on metallic substrates such as 6061 aluminum alloy [1]. However, maintaining long-term joint integrity under sustained thermal exposure remains a significant challenge in aerospace, automotive, and electronic applications where service temperatures routinely exceed 100–150 °C [2, 3].

Incorporating inorganic fillers is a proven strategy to simultaneously enhance the thermal stability, mechanical performance, and interfacial adhesion of epoxy matrices [4, 5]. Various fillers have been investigated, including Al for thermal conductivity and CTE compatibility [6, 7]; ZrO_2 for thermal stability and corrosion resistance [8, 9]; TiO_2, TiC, and WC for wear and structural integrity at elevated temperatures [10, 11]; and h-BN for exceptional in-plane thermal conductivity combined with dielectric properties [12, 13].

To further strengthen interfacial adhesion, silane coupling agents (SCAs) are widely employed. Rather than pre-treating the fillers, incorporating silanes directly into the adhesive via the integral blend method (in-situ modification) allows the agent to simultaneously modify the filler surface

and reinforce adhesion to the metal substrate during curing [14]. This study systematically evaluates the effect of different organofunctional silanes (APTMS, GPTMS, VTMS) and six microparticulate fillers on the initial lap shear strength and 500-h thermal aging durability (at 80 °C) of an epoxy/polyamide system [15, 16], providing scientific guidelines for formulating highly durable structural adhesives.

2. EXPERIMENTAL

2.1. Materials

The matrix comprised DGEBA epoxy resin (YD-128S, EEW = 184–190 g/eq) and polyamide hardener (G-5022, amine value = 220–240 mg KOH/g) from Kukdo Chemical. Six fillers were used: ZrO_2 (1–5 μm), Al (≤15 μm), TiC (<4 μm), WC (~2 μm), h-BN (~1 μm), and rutile TiO_2 (<5 μm). Three silanes (APTMS, GPTMS, VTMS; 97–98% purity) were obtained from Sigma-Aldrich. The substrate was 3 mm thick 6061-T6 aluminum alloy.

2.2. In-situ modification and specimen preparation

The experimental program was conducted in two stages. Stage 1 investigated the effect of ZrO_2 content (0–7.5 wt%) without silane. Stage 2 fixed the optimum filler content (5.0 wt%) and evaluated three silanes; the best silane was then applied across all six filler systems. The full sample matrix is presented in Table 1.

Table 1. *Adhesive formulations investigated in this study.*

No.	Sample designation	Filler type	Filler content (wt%)	Silane agent
1	REF	None	0	None
2	Z-2.5	ZrO_2	2.5	None
3	Z-5.0	ZrO_2	5.0	None
4	Z-7.5	ZrO_2	7.5	None
5	Z-5.0-A	ZrO_2	5.0	APTMS
6	Z-5.0-G	ZrO_2	5.0	GPTMS
7	Z-5.0-V	ZrO_2	5.0	VTMS
8	Al-5.0-APTMS	Al	5.0	APTMS
9	TiO_2-5.0-APTMS	TiO_2	5.0	APTMS
10	WC-5.0-APTMS	WC	5.0	APTMS
11	TiC-5.0-APTMS	TiC	5.0	APTMS
12	BN-5.0-APTMS	BN	5.0	APTMS

The epoxy resin was preheated to 60 °C to facilitate dispersion. The filler was introduced and mixed via mechanical stirring (2,000 rpm, 30 min), followed by ultrasonic homogenization (15 min, 40% amplitude). After cooling to room temperature, the silane agent (1.0 wt% relative to filler mass) was blended for 20 min to allow in-situ hydrolysis and condensation. Finally, the polyamide hardener was added at a stoichiometric ratio. Lap shear specimens (ASTM D1002, 12.5 mm overlap, 0.25 mm bondline) were prepared using abraded and degreased 6061-T6 coupons. Joints were cured at 23 ± 2 °C for 24 h and post-cured at 80 °C for 4 h.

2.3. Characterization

Initial lap shear strength (LSS_0) and strength after isothermal aging at 80 °C (for 168 h, 336 h, and 500 h) were measured using a universal testing machine (Instron 5969, USA) at 1.3 mm/min.

The thermal retention factor (TRF) was calculated as (LSS_aged / LSS_initial) × 100%. Fracture morphology was examined via SEM (JEOL JSM-6490, Japan). Thermal decomposition was analyzed by TGA/DTG (TA Instruments Q500, USA) in air from 25 to 840 °C at 10 °C/min.

3. RESULTS AND DISCUSSION

3.1. Effect of ZrO_2 content on lap shear strength

As illustrated in Figure 1, LSS_0 increased from 8.7 ± 0.6 MPa for the unfilled reference (REF) to a maximum of 12.4 ± 0.8 MPa at 5.0 wt% ZrO_2 (Z-5.0), owing to effective stress transfer and crack deflection by well-dispersed particles. However, at 7.5 wt% (Z-7.5), particle agglomeration induced stress concentrators, reducing LSS_0 to 11.1 ± 1.2 MPa. Thermal aging confirmed this trend (Figure 1). The Z-5.0 formulation retained the highest strength (LSS_{500h} = 10.3 MPa, TRF = 83.1%).

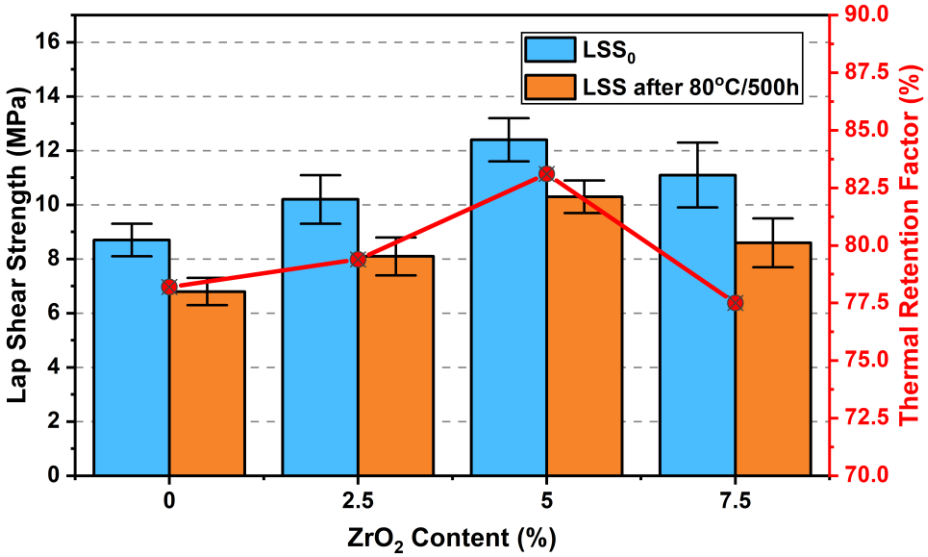

Figure 1. *Initial LSS_0 and TRF of epoxy adhesives as a function of ZrO_2 filler content. Error bars represent one standard deviation (n = 5).*

Conversely, Z-7.5 exhibited the lowest TRF (77.5%), falling below the REF (78.2%). Agglomerated particle clusters in highly filled systems create preferential microvoid channels that facilitate oxygen diffusion and thermal stress relaxation, accelerating interfacial bond degradation. Consequently, 5.0 wt% was fixed for subsequent silane evaluations.

3.2. Effect of silane coupling agent type

Using 5.0 wt% ZrO_2, three in-situ silanes were evaluated, and the comparative results are presented in Figure 2. APTMS significantly outperformed GPTMS, VTMS, and the silane-free system, yielding LSS_0 = 15.6 MPa (a 25.8% increase over Z-5.0) and an outstanding TRF of 88.5% (LSS_{500h} = 13.8 MPa). Notably, APTMS exhibited the lowest degradation rate, losing only 0.3 MPa between 168 h and 500 h, indicating a highly stable interfacial equilibrium. GPTMS showed intermediate performance (LSS_0 = 13.8 MPa, TRF = 82.6%), while VTMS yielded the lowest results (LSS_0 = 11.6 MPa, TRF = 79.3%). This divergence highlights the critical role of chemical reactivity under ambient "cold-cure" conditions (23 °C for 24 h). The primary amine groups of APTMS are highly reactive toward DGEBA epoxy rings at room temperature, ensuring rapid and robust integration into the crosslinked network. In contrast, GPTMS's glycidoxy groups require elevated temperatures for complete ring-opening, resulting in a less stable interphase. The superior performance of APTMS stems from its dual bonding mechanism: continuous covalent linkages from the bulk polymer, through the silane interphase, to both the filler surface (Si–O–Zr) and the aluminum substrate (Si–O–Al).

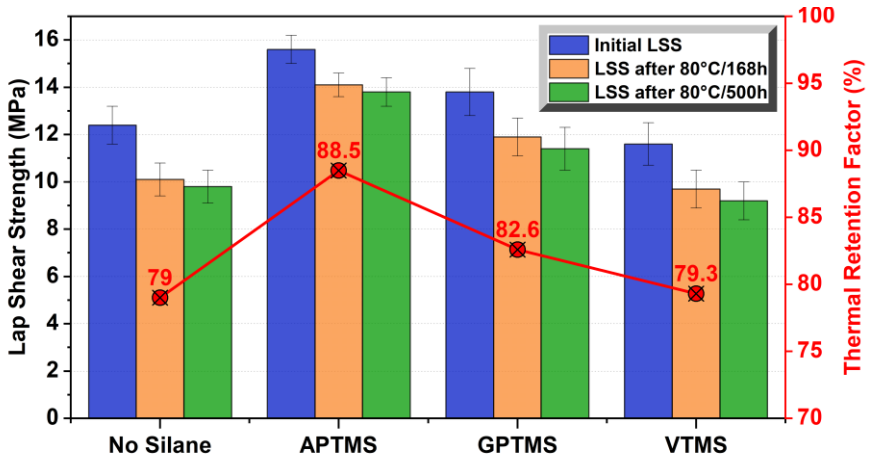

Figure 2. *Effect of different silane coupling agents on the initial LSS and TRF of ZrO_2-5.0 systems. Error bars represent one standard deviation (n = 5). TRF values corresponding to the 500 h aging interval are indicated on the figure.*

3.3. Comparative performance of different filler systems

Table 2 and Figure 3 summarize the comparative performance of the six inorganic systems with 1.0 wt% APTMS and 5.0 wt% filler loading. Evaluated against dual criteria ($LSS_0 \geq 15$ MPa and TRF-500h ≥ 85%), four systems qualified: h-BN, WC, ZrO_2, and TiC. As detailed in Table 2, the highest LSS_0 values were recorded for WC (16.1 MPa), h-BN (15.9 MPa), and ZrO_2 (15.6 MPa). WC and TiC primarily stiffened the matrix via high hardness, whereas ZrO_2 formed strong silane-mediated networks due to its high surface hydroxyl density.

Table 2. *Lap shear strength and thermal retention factor of adhesive systems as a function of filler type (6061 Al alloy substrate, APTMS 1.0 wt%, thermal aging at 80 °C).*

Sample	Filler	LSS_0 (MPa)	LSS_{500h} (MPa)	TRF-500h (%)	Assessment
REF	—	8,7 ± 0,6	6,8 ± 0,5	78,2	Fail
Z-5.0-APTMS	ZrO_2	15,6 ± 0,6	13,8 ± 0,6	88,5	Pass
Al-5.0-APTMS	Al	13,4 ± 0,9	10,7 ± 0,9	79,9	Fail
Ti-5.0-APTMS	TiO_2	11,2 ± 1,0	8,8 ± 0,9	78,6	Fail
WC-5.0-APTMS	WC	16,1 ± 0,8	13,9 ± 0,7	86,3	Pass
TC-5.0-APTMS	TiC	14,8 ± 0,9	12,6 ± 0,8	85,1	Pass
BN-5.0-APTMS	h-BN	15,9 ± 0,7	14,5 ± 0,6	90,6	Pass

Regarding thermal aging (Figure 3), h-BN-5.0-APTMS achieved the highest stability (TRF = 90.6%, LSS_{500h} = 14.5 MPa). Although WC has superior bulk thermal stability, h-BN's unique lamellar (platelet) morphology creates an exceptional "tortuosity effect," physically extending the diffusion path for oxygen and moisture. Furthermore, h-BN's high intrinsic thermal conductivity (~300 W/m·K) facilitates local heat dissipation, preventing localized degradation at the bonding interface. Conversely, Al-5.0-APTMS failed the criteria (TRF = 79.9%, LSS_{500h} = 10.7 MPa). This continuous degradation is attributed to the progressive oxidation of Al particles (forming Al_2O_3, Pilling–Bedworth ratio > 1) and a significant mismatch in the Coefficient of Thermal Expansion (CTE) between the Al particles (~23×10^{-6}/K) and the epoxy matrix (~$60–80\times10^{-6}$/K). During

prolonged 80 °C exposure, this CTE disparity generates persistent thermal stresses, inducing micro-cracks that compromise joint integrity. TiO_2-5.0-APTMS exhibited the lowest strength retention (TRF = 78.6%), reflecting poor interfacial silane condensation due to its lower surface hydroxyl density.

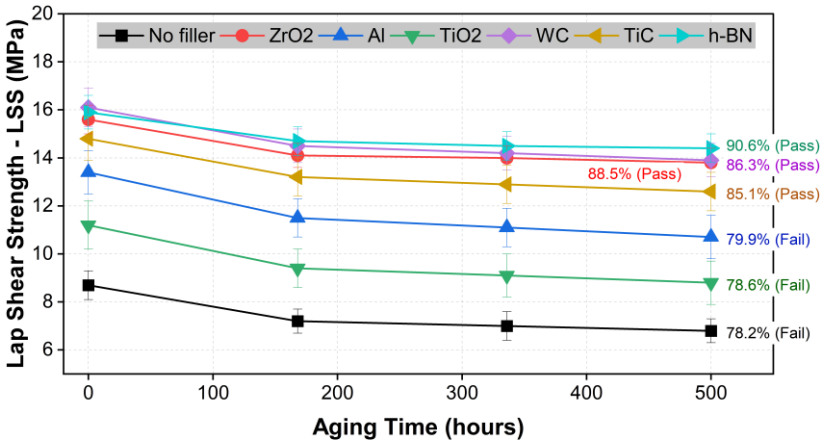

Figure 3. *Lap shear strength as a function of thermal aging time (80 °C, 0–500 h) for seven epoxy/polyamide adhesive systems on 6061 aluminum alloy substrates. Lines represent mean values (n = 5). TRF-500h values and Pass/Fail assessments according to the dual qualification criterion are indicated at the terminal data point of each curve.*

3.4. Fracture surface morphology (SEM)

The fracture surface morphologies presented in Figure 4 provide mechanistic support for the mechanical data. After tensile testing, the unfilled REF specimen (Figure 4a) exhibited a classic adhesive failure mode (<5% cohesive fraction), which corresponds directly to its low initial strength (8.7 MPa). The silane-free Z-7.5 system (Figure 4b) showed severe particle agglomerates (1–3 µm clusters) and interfacial voids. These agglomerates act as stress concentrators and create micro-pathways that facilitate oxygen diffusion, thereby explaining the sharp decline in its thermal retention factor.

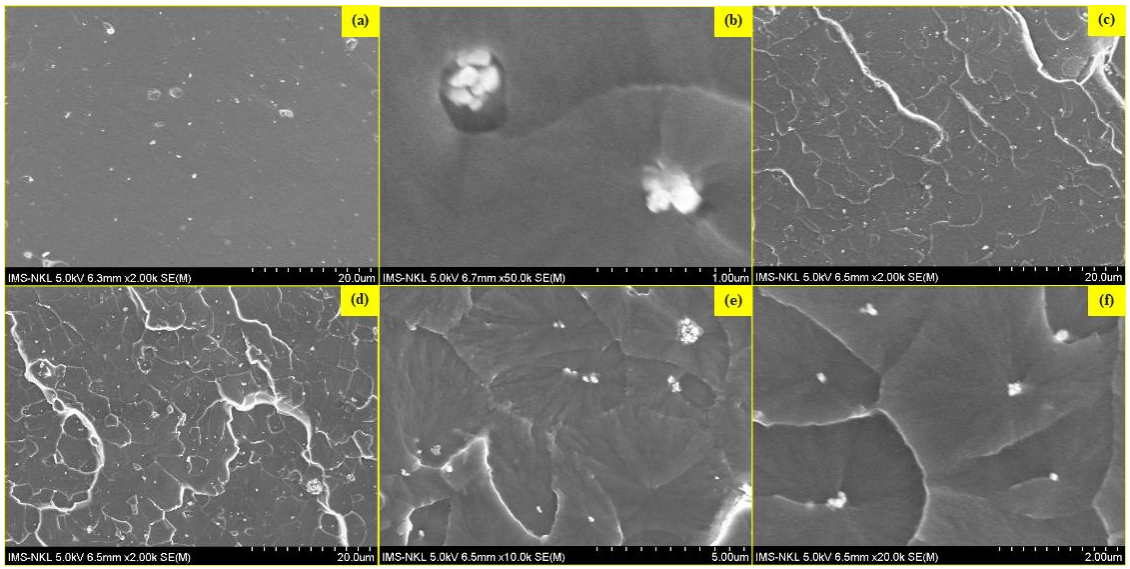

Figure 4. *SEM images of fracture surfaces of lap shear specimens after tensile testing: (a) REF, (b) silane-free Z-7.5, and APTMS-modified systems including (c, d) ZrO_2-5.0-APTMS and (e, f) BN-5.0-APTMS.*

In contrast, the APTMS-modified systems (Figure 4c, d for ZrO_2-5.0-APTMS and Figure 4e, f BN-5.0-APTMS, respectively) displayed a pronounced shift toward mixed and cohesive failure modes (62–71% cohesive fraction). River-mark patterns were clearly observed, indicating effective fracture energy dissipation through the adhesive bulk rather than at the interface. Filler particles were uniformly distributed without large clusters, and the filler–polymer interfaces remained completely intact even after 500 h of thermal aging. These morphological features physically validate the critical role of APTMS in forming a robust, continuous covalent network that effectively protects the bonding interface against thermo-oxidative degradation.

3.5. Thermogravimetric analysis (TGA/DTG)

The bulk thermo-oxidative decomposition behavior is evaluated via TGA and DTG in air, with curves presented in Figures 5 and 6 and parameters summarized in Table 3. All filled systems exhibited higher 5% mass loss temperatures (T_5%) than the unfilled REF (323 °C), following the order: WC (341 °C) > BN (339 °C) > TiC (337 °C) > ZrO_2 (331 °C) > Al (329 °C) > TiO_2 (325 °C). This confirms the oxygen diffusion barrier effect, where dispersed particles retard oxidative degradation. As shown in the DTG curves (Figure 6), BN-5.0-APTMS exhibited the highest secondary decomposition peak (Tmax2 = 436 °C), further demonstrating the efficacy of its lamellar barrier and thermal dissipation properties.

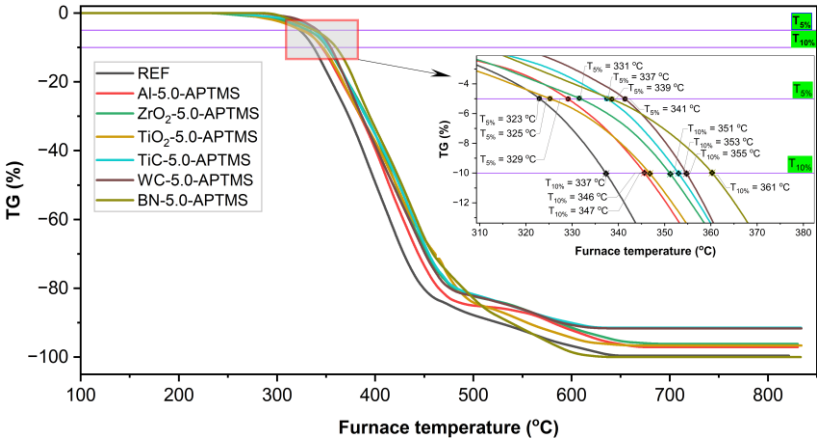

Figure 5. *TGA curves of seven polyamide cured epoxy adhesive systems.*

Table 3. *Thermal decomposition parameters of adhesive systems determined from TGA/DTG in air.*

Mẫu	T_5% (°C)	T_{10}% (°C)	T_{max1} (°C)	T_{max2} (°C)	Char 800°C (%)
REF	323	337	356	400	0
Al-5.0-APTMS	329	346	364	413	2.90
ZrO_2-5.0-APTMS	331	351	366	417	3.86
TiO_2-5.0-APTMS	325	347	375	420	3.41
TiC-5.0-APTMS	337	353	374	433	8.56
WC-5.0-APTMS	341	355	392	—	8.37
BN-5.0-APTMS	339	361	389	436	0.04

According to Table 3, char yields at 800 °C matched expectations for WC (8.37%) and TiC (8.56%). The ZrO_2 char yield (3.86%) was slightly lower than the nominal 5.0 wt% loading; this discrepancy is attributed to the volatilization of physically bound water and surface hydroxyls, the

complete decomposition of the organic APTMS layer (1.0 wt%), and minor local dispersion variances within the small TGA sample mass (~10 mg). The h-BN system yielded near-zero char (0.04%) due to the high-temperature oxidation of h-BN into volatile B_2O_3, though this does not negate its superior barrier performance at lower service temperatures (< 440 °C). Importantly, T_5% (bulk degradation > 300 °C) does not strictly correlate with TRF (interfacial degradation at 80 °C). While WC has the highest T_5%, h-BN provides the best TRF, proving that long-term moderate-temperature durability is governed by interfacial integrity and tortuosity rather than absolute decomposition temperature.

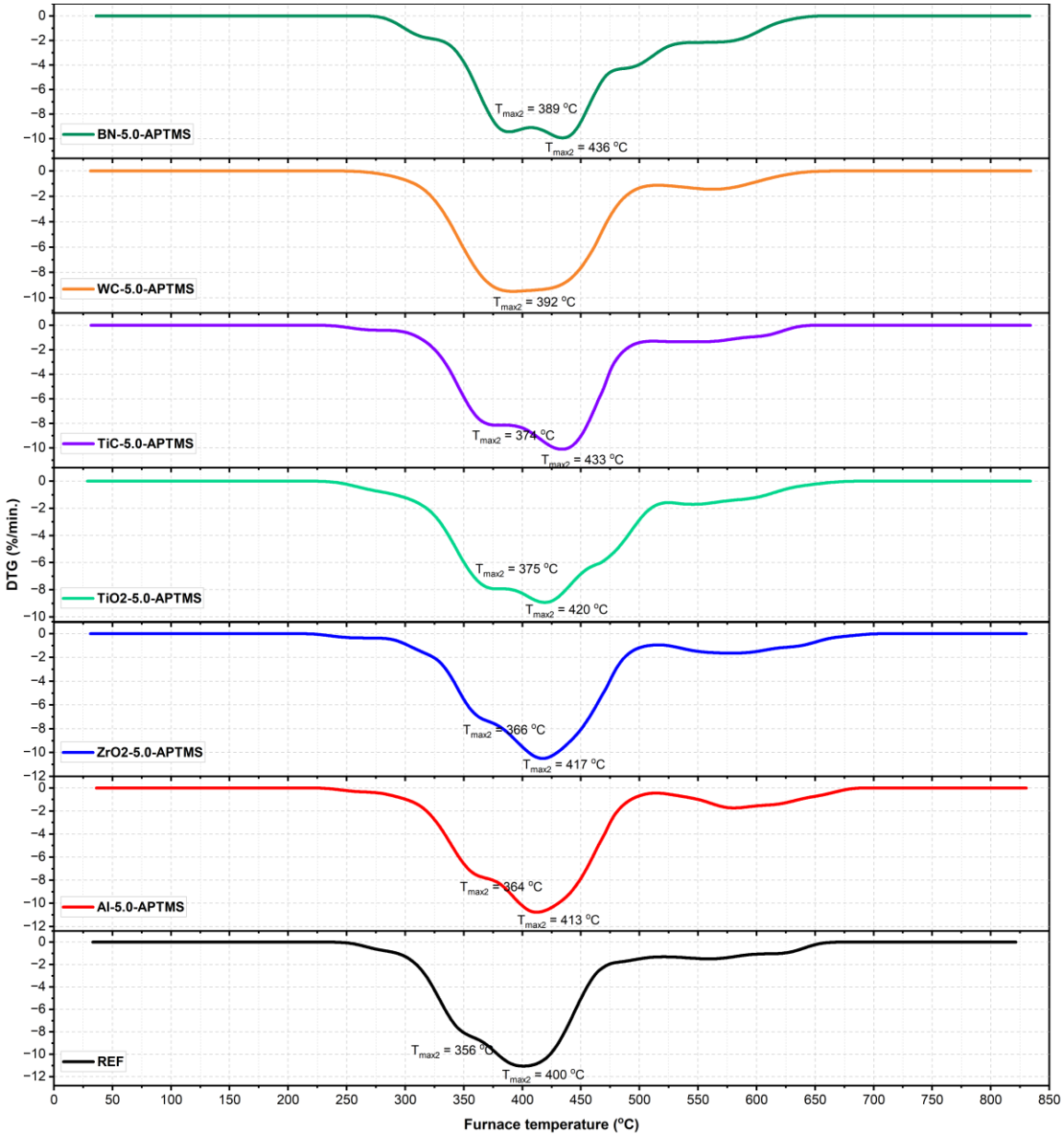

Figure 6. *DTG curves of seven polyamide cured epoxy adhesive systems.*

4. CONCLUSIONS

This study demonstrated that an optimal filler loading of 5.0 wt% combined with 1.0 wt% in-

situ APTMS modification significantly enhances the mechanical performance and thermal durability of epoxy/polyamide joints on aluminum substrates. Under ambient "cold-cure" conditions, APTMS outperformed GPTMS and VTMS due to the high reactivity of its primary amine groups, creating a continuous and highly stable Si–O–Metal/Filler and amine–epoxy covalent network. When evaluated against the dual criteria of initial lap shear strength ($LSS_0 \geq 15$ MPa) and thermal retention factor after 500 hours (TRF-500h ≥ 85%), h-BN, WC, ZrO_2, and TiC emerged as highly viable structurally durable fillers. Among them, the h-BN-5.0-APTMS system provided the best overall performance, achieving an $LSS_{500}h$ of 14.5 MPa and a TRF of 90.6%. This superior aging resistance is driven by the unique lamellar structure of h-BN, which induces a strong tortuosity effect to block oxygen diffusion and facilitates rapid thermal dissipation, thereby protecting the bonding interface. Conversely, systems incorporating Al particles suffered continuous strength loss during aging due to oxidation-induced volume expansion and severe CTE mismatch with the polymer matrix. Finally, thermogravimetric analysis (TGA/DTG) confirmed that inorganic fillers actively retard high-temperature thermo-oxidative decomposition by acting as effective oxygen diffusion barriers. These findings provide a robust scientific basis for formulating long-term, high-temperature resistant structural adhesives.

Acknowledgement: *This paper was funded by project NCPTVL.07/25-26*

REFERENCES

[1]. Jin, F.-L., X. Li, and S.-J. Park. *"Synthesis and application of epoxy resins: A review"*. Journal of Industrial and Engineering Chemistry, vol. 29, pp. 1–11, (2015).

[2]. Cavezza, F., et al. *"A Review on Adhesively Bonded Aluminium Joints in the Automotive Industry"*. Metals, vol. 10, No. 6, pp. 730, (2020).

[3]. Rudawska, A., et al. *"Modification of Epoxides with Metallic Fillers-Mechanical Properties after Ageing in Aqueous Environments"*. Materials (Basel), vol. 16, No. 22, (2023).

[4]. Samantaray, R., et al. *"Effect of Different Inorganic Fillers on the Physical and Mechanical Properties of Bisphenol-A Epoxy Matrix"*. Polymer Engineering & Science, vol. 66, No. 4, pp. 2960-2977, (2026).

[5]. Nassar, A., et al. *"Improved Wear-Resistant Performance of Epoxy Resin Composites Using Ceramic Particles"*. Polymers, vol. 14, No. 2, pp. 333, (2022).

[6]. Choi, S.W., K.H. Yoon, and S.-S. Jeong. *"Morphology and thermal conductivity of polyacrylate composites containing aluminum/multi-walled carbon nanotubes"*. Composites Part A: Applied Science and Manufacturing, vol. 45, pp. 1–5, (2013).

[7]. Kim, J.S., et al. *"Mechanical Properties and Thermal Conductivity of Epoxy Composites Containing Aluminum-Exfoliated Graphite Nanoplatelets Hybrid Powder"*. Macromolecular Research, vol. 29, No. 3, pp. 252–256, (2021).

[8]. Wu, J., G. Ji, and Q. Wu. *"Preparation of epoxy/ZrO2 composite coating on the Q235 surface by electrostatic spraying and its corrosion resistance in 3.5% NaCl solution"*. RSC Advances, vol. 12, No. 17, pp. 10625–10633, (2022).

[9]. Samad, U.A., et al. *"Synergistic Effect of Nanoparticles: Enhanced Mechanical and Corrosion Protection Properties of Epoxy Coatings Incorporated with SiO2 and ZrO2"*. Polymers, vol. 15, No. 14, pp. 3100, (2023).

[10]. Alsaeed, T., et al. *"Mechanical and Tribological Performance of Epoxy Composites Reinforced with YSZ Waste Ceramics for Sustainable Green Engineering Applications"*. Processes, vol. 12, No. 11, pp. 2609, (2024).

[11]. Ghani, S.N., A.S. Alithari, and H.S. Hasan. *"Influence of adding tungsten carbide and titanium dioxide nanoparticles on the impact strength of epoxy based composite materials used in marine applications"*. Results in Engineering, vol. 25, pp. 104012, (2025).

[12]. Lee, E.-S., et al. *"High thermal conductivity of boron nitride filled epoxy composites prepared by tin solder nanoparticle decoration"*. Composites Part B: Engineering, vol. 225, pp. 109264, (2021).

[13]. Meng, Y., et al. *"Thermal Conductivity Enhancement of Polymeric Composites Using Hexagonal Boron Nitride: Design Strategies and Challenges"*. Nanomaterials, vol. 14, No. 4, pp. 331, (2024).

[14]. España, J.M., et al. *"Investigation of the effect of different silane coupling agents on mechanical performance of basalt fiber composite laminates with biobased epoxy matrices"*. Polymer Composites, vol. 34, No. 3, pp. 376–381, (2013).
[15]. Liu, H., et al. *"Enhancing interfacial properties of epoxy coatings via hyperbranched modification of SiC fillers: Experimental and simulation insights"*. Chemical Engineering Journal, vol. 511, pp. 161841, (2025).
[16]. Zaferani, S.H., et al. *"The effect of organosilane on corrosion resistance of epoxy coating containing cerium nitrate"*. Journal of Adhesion Science and Technology, vol. 28, No. 2, pp. 151–160, (2014).

TÓM TẮT

Ảnh hưởng của loại chất độn vô cơ và biến tính silane in-situ đến độ bền kéo trượt và độ bền lão hóa nhiệt của hệ keo epoxy/polyamide trên nền hợp kim nhôm

Nghiên cứu khảo sát ảnh hưởng của loại và hàm lượng chất độn vô cơ (ZrO_2, Al, TiO_2, TiC, WC, h-BN) kết hợp tác nhân silane biến tính in-situ (APTMS, GPTMS, VTMS) đến độ bền kéo trượt và độ ổn định nhiệt của hệ keo epoxy/polyamide trên nền hợp kim nhôm 6061. Hàm lượng ZrO_2 tối ưu xác định là 5,0% khối lượng, cho LSS_0 = 12,4 MPa và TRF-500h = 83,1% khi không sử dụng silane. APTMS là tác nhân silane hiệu quả nhất nhờ cơ chế liên kết kép tại giao diện, nâng LSS_0 lên 15,6 MPa và TRF-500h lên 88,5% cho hệ ZrO_2-5.0-APTMS. Đánh giá sáu hệ chất độn theo tiêu chí kép $LSS_0 \geq 15$ MPa và TRF-500h ≥ 85% xác định bốn hệ đạt yêu cầu là h-BN, WC, ZrO_2 và TiC, trong đó, h-BN-5.0-APTMS tối ưu nhất với TRF = 90,6% và $LSS_{500}h$ = 14,5 MPa nhờ hiệu ứng đường dẫn ngoằn ngoèo và khả năng tản nhiệt của cấu trúc dạng lớp. Phân tích TGA/DTG trong không khí xác nhận tất cả các hệ chứa chất độn có T_5% cao hơn mẫu đối chứng (REF: 323 °C) theo thứ tự WC (341 °C) > BN (339 °C) > TiC (337 °C) > ZrO_2 (331 °C) > Al (329 °C) > TiO_2 (325 °C), theo cơ chế hàng rào khuếch tán oxy. Kết quả cung cấp cơ sở khoa học cho việc phát triển hệ keo epoxy/polyamide biến tính ứng dụng trong các kết cấu yêu cầu độ bền cơ lý cao và ổn định nhiệt dài hạn.

Từ khoá: Keo epoxy/polyamide; Chất độn vô cơ; Silane APTMS; Độ bền kéo trượt; Lão hóa nhiệt.